Hybridization of fluorescein-labeled DNA oligomers detected by fluorescence anisotropy with protein binding enhancement

ARTICLE *in* ANALYTICAL CHEMISTRY · DECEMBER 1995

Impact Factor: 5.64 · DOI: 10.1021/ac00117a020 · Source: PubMed

5 AUTHORS, INCLUDING:

George Li
Memorial Sloan-Kettering Cancer Center
71 PUBLICATIONS **582** CITATIONS
SEE PROFILE

Linda Mcgown
Rensselaer Polytechnic Institute
160 PUBLICATIONS **3,094** CITATIONS
SEE PROFILE

Hybridization of fluorescein-labeled DNA oligomers detected by fluorescence anisotropy with protein binding enhancement

Michael U. Kumke, Guang. Li, Linda B. McGown, G. Terrance. Walker, and C. Preston. Linn

Anal. Chem., **1995**, 67 (21), 3945-3951 • DOI: 10.1021/ac00117a020

Anal. Chem. **1995**, *67*, 3945–3951

Hybridization of Fluorescein-Labeled DNA Oligomers Detected by Fluorescence Anisotropy with Protein Binding Enhancement

Michael U. Kumke, Guang Li, and Linda B. McGown*

P. M. Gross Chemical Laboratory, Department of Chemistry, Duke University, Box 90346, Durham, North Carolina 27708-0346

G. Terrance Walker* and C. Preston Linn

Becton Dickinson and Company Research Center, Research Triangle Park, North Carolina 27709

Fundamental aspects of the application of fluorescence anisotropy to detect the hybridization of fluorescein-labeled DNA oligomers were explored. The oligomers included a binding site for the *Eco*RI restriction enzyme, which binds to double-stranded DNA and is used in this work to enhance the difference between the anisotropies of the single-stranded and double-stranded oligomers by increasing the effective volume of the latter. The fluorescence anisotropy increases upon hybridization and further upon binding of *Eco*RI to the double strand. By varying the length of the tether used to attach the fluorescein to the 5′ end of the oligonucleotide, it was found that a 6-carbon tether was optimal, providing the most dramatic increases in anisotropy in the presence of *Eco*RI. Dynamic fluorescence anisotropy (DFA) provided insight into the increases in steady-state anisotropy. In most cases, the best fits to the DFA data were obtained using a biexponential decay model, which describes an anisotropic rotator. Upon hybridization, the faster rotational motion is more hindered, and the contribution of the slower rotational component is increased. This effect is enhanced by binding of *Eco*RI to the double strand, especially when the *Eco*RI binding site is near the fluorescein at the 5′ end and the tether length is in the optimal range. Because the rotational correlation time of the slower anisotropy decay component is much longer than the fluorescence lifetime, it is possible in some cases to reduce the anisotropic rotator model to the special limiting case of a hindered rotator.

Detection of DNA sequences has important applications in clinical diagnostics. A simple and direct approach is to probe the unknown DNA specimen with probe DNA of a known sequence and monitor the occurrence of hybridization using separation techniques. These separation techniques, however, are time consuming and sensitive to experimental conditions. A big improvement would be the ability to monitor the hybridization process in situ without a physical separation.[1-6]

Fluorescence spectroscopic methods offer high sensitivity and selectivity, combined with the potential for nonseparation, in situ applications. Among these methods, steady-state and dynamic fluorescence anisotropy have proven to be particularly useful for monitoring molecular motions, such as rotations of proteins and reorientations of molecules in membranes or macromolecular structures.[7-10] Due to the dependence of these molecular motions on molecular size, fluorescence anisotropy offers the potential for monitoring DNA hybridization.

This paper describes the detection of DNA hybridization through measurements of the fluorescence anisotropy of fluorescein that is covalently tethered to the oligomers. By applying steady-state fluorescence anisotropy, we were able to monitor the DNA hybridization in situ without a prior separation step. The incorporation of a binding site for the *Eco*RI restriction enzyme into the oligomers provided a mechanism for enhanced detection of hybridization, since *Eco*RI binds only to the double-stranded DNA. Thus, the increase in anisotropy observed when the fluorescein-labeled oligomer undergoes hybridization is enhanced by the binding of *Eco*RI to the double strand. The hybridization and *Eco*RI binding are depicted in Figure 1.

Dynamic fluorescence anisotropy (DFA) provided further insight into the mechanisms that are responsible for the increases in anisotropy that occur upon hybridization and *Eco*RI binding, through measurements of oligomers with different tether lengths and different positions for the *Eco*RI binding site relative to the tethered fluorescein. Results of fluorescence lifetime measurements, which are necessary for the DFA analysis, are described as well.

EXPERIMENTAL SECTION

Materials. DNA33-4C-5′, DNA33-9C-5′, and DNA33-12C-5′ were synthesized and purified by Molecular Probes (Eugene, OR).

(1) Mathies, R. A.; Zhu, H.; Clark, S. M.; Benson, S. C.; Rye, H. S.; Glazer, A. N. *Anal. Chem.* **1994**, *66*, 1941.
(2) Netzel, T. L.; Telser, J.; Cruickshank, K. A.; Morrison, L. E. *J. Am. Chem. Soc.* **1989**, *111*, 6966.
(3) Schwartz, H. E.; Ulfelder, K. J. *Anal. Chem.* **1992**, *64*, 1737.
(4) Seeger, S.; Galla, K.; Arden-Jacob, J.; Deltau, G.; Drexhage, K. H.; Martin, M.; Sauer, M.; Wolfrum, J. *J. Fluoresc.* **1994**, *4*, 111.
(5) Seeger, S.; Sauer, M.; Han, K.-T.; Mueller, R.; Schulz, A.; Tadday, R.; Wolfrum, J.; Arden-Jacob, J.; Deltau, G.; Marx, N. J.; Drexhage, K. H. *J. Fluoresc.* **1993**, *3*, 131.
(6) Vo-Dinh, T.; Houck, K.; Stokes, D. L. *Anal. Chem.* **1994**, *66*, 3379.
(7) Fleming, G. R.; Petrich, J. W.; Longworth, J. W. *Biochemistry* **1987**, *26*, 2711.
(8) Lakowicz, J. R.; Gryczynski, I. *J. Fluoresc.* **1992**, *2*, 117.
(9) Lakowicz, J. R.; Bucci, E.; Gryczynski, Z.; Fronticelli, C.; Gryczynski, I. *J. Fluoresc.* **1992**, *2*, 29.
(10) Stryer, L.; Munro, I.; Pecht, I. *Proc. Natl. Acad. Sci. U.S.A.* **1979**, *76*, 56.

0003-2700/95/0367-3945$9.00/0

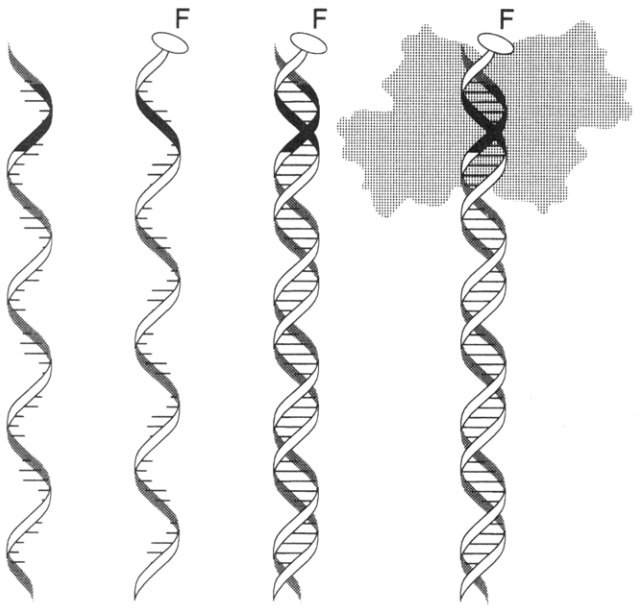

Figure 1. Depiction of (left to right) a single-stranded oligomer, hybridization to form a double strand, and *Eco*RI binding to the double strand at the 5′ end. The schematic representation of *Eco*RI bound to the fluorescein-labeled DNA oligomer is based on the X-ray crystal structure of *Eco*RI bound to DNA[23] as deposited in the Protein Data Bank (PDB).[24,25] F denotes the fluorescein that is tethered to the 5′ end.

Set I (location of binding site varied)

DNA28-6C-3' : ^{5}F-TGAAAGACGTTGAATTCCATACGGATAG

DNA28-6C-5' : ^{5}F-GGAATTCAGTTATCCACCATACGGATAG

DNA28-6C-mid : ^{5}F-TGAAAGAATTCATCCACCATACGGATAG

Set II (tether length varied)

DNA33-4C-5' : ^{5}F-GGAATTCATCCGTATGGTGGATAACGTCTTTCA

DNA33-6C-5' : ^{5}F-GGAATTCATCCGTATGGTGGATAACGTCTTTCA

DNA33-9C-5' : ^{5}F-GGAATTCATCCGTATGGTGGATAACGTCTTTCA

DNA33-12C-5' : ^{5}F-GGAATTCATCCGTATGGTGGATAACGTCTTTCA

Figure 2. Sequences of the DNA oligomers. The *Eco*RI binding site (GAATTC) is underlined.

The other oligodeoxynucleotides were synthesized by an ABI Model 380B synthesizer (Applied Biosystems Division, Perkin Elmer, Norwalk, CT) and purified by denaturing gel electrophoresis. The oligodeoxynucleotides are described in Figure 2 and Table 1. Homogeneous preparations of the oligonucleotides were confirmed by observation of a single band upon gel electrophoresis analysis. 5′-Fluorescein-labeled oligodeoxynucleotides were prepared by standard procedures using the reagent 6-FAM Amidite from Applied Biosystems Inc. (P/N 401527) according to the product insert protocols. Chemical structures of the various tethers used to link the fluorescein label (F) to the DNA oligomers are as follows: 4C, F−CONH$(CH_2)_3$−OPO_2−DNA(5′−3′); 6C, F−CONH$(CH_2)_5OPO_2$−DNA(5′−3′); 9C, F−CONH$(CH_2)_5$CNH-$(CH_2)_3OPO_2$−DNA(5′−3′); 12C, F−CONH$(CH_2)_5$CNH$(CH_2)_5$-OPO_2−DNA(5′−3′). The samples were purified by oligonucleotide purification cartridge and standard gel purification. Oligomer concentrations were determined using the molar absorptivity at 260 nm. The absorbances of the labeled oligomers were corrected for fluorescein contributions at 260 nm by subtraction of one-fifth of the fluorescein absorbance at 496 nm. Unless otherwise stated, the concentration of oligomer in the samples was 5×10^{-8} M.

Table 1. Summary of the DNA Oligomers Used in This Work[a]

sample	no. of nucleotides	tether length	location of *Eco*RI binding site
		Set I	
DNA28-6C-5′	28	6	1 nucleotide from tether
DNA28-6C-mid	28	6	6 nucleotides from tether
DNA28-6C-3	28	6	11 nucleotides from tether
		Set II	
DNA33-4C-5	33	4	1 nucleotide from tether
DNA33-6C-5	33	6	1 nucleotide from tether
DNA33-9C-5	33	9	1 nucleotide from tether
DNA33-12C-5	33	12	1 nucleotide from tether

[a] Set I consists of 28-mers with a 6-carbon tether to fluorescein; the *Eco*RI binding site is varied. Set II consists of 33-mers in which the binding site is one nucleotide removed from the 5′ end; the tether length is varied.

The *Eco*RI restriction enzyme (*Eco*RI 101 CXL, New England BioLabs) was purchased at a concentration of 100 000 units/mL. The experiments with *Eco*RI were performed at a concentration of 2500 units/mL. All experiments were performed in a buffer solution containing 100 mM Tris-HCl (pH 7.5), 0.6 mM K_2PO_4 (pH 7.5), 50 mM NaCl, 6% glycerol, 1 mM EDTA, 24 μg/mL bovine serum albumin (BSA), 0.02% Triton X-100, and 0.6 mM β-mercaptoethanol. The K_2PO_4, glycerol, BSA, Triton X-100, and β-mercaptoethanol were contributed by the stock *Eco*RI solution. Experiments lacking *Eco*RI also contained these reagents. The *Eco*RI cleavage of the DNA upon hybridization is inhibited by inclusion of EDTA, which chelates the cofactor Mg^{2+}.

Methods. *Steady-State Anisotropy Measurements.* Steady-state anisotropy measurements were performed using a phase-modulation spectrofluorometer (Model 48000S, SLM instruments, Inc.) in the steady-state mode, in the L-format configuration. Excitation at 488 nm was provided by passing the output of a 450 W xenon arc lamp through a monochromator with the entrance and exit slits set to a bandpass of 4 nm.

Fluorescence anisotropy was measured with the same instrument using the L-format configuration,[11] in which the anisotropy (r) is calculated from measurements of the emission intensity, I, according to

$$r = \frac{I_{vv} - I_{vh}G}{I_{vv} + 2I_{vh}G} \quad (1)$$

where the subscripts v and h refer to the orientation (vertical or horizontal) of the polarizers in the excitation beam (first subscript) and the emission beam (second subscript) for that intensity measurement. The instrumental correction factor, G, is equal to the ratio of I_{hv} to I_{hh}.

Fluorescence Lifetime and Dynamic Anisotropy Measurements. Fluorescence lifetime and dynamic anisotropy measurements were performed in the frequency domain,[11] using a multiharmonic Fourier transform spectrofluorometer (Model 4850 MHF, SLM

(11) Lakowicz, J. R. *Principles of Fluorescence Spectroscopy*; Plenum Press: New York, 1983.

Instruments Inc.).[12] A base frequency of 4.1 MHz and a correlation frequency of 7.292 Hz were used in all experiments. Data at 50 modulation frequencies ranging from the base frequency up to 205 MHz were used in the analyses. Each measurement consisted of 15 (or, in some cases, 10) pairs of sample–reference measurements, each of which was the internal average of 100 samplings. An air-cooled argon laser (Model 543, Omnichrome) was used to provide excitation at 488 nm. The laser output power was set to 50 mW (~40% of maximal output power) and was controlled by an internal laser power meter. The sample compartment was maintained at 25 ± 0.1 °C with a water circulating thermostat. Emission wavelength selection was achieved using a combination of a 520 nm long-pass filter (Oriel) and a 560 nm short-pass filter (CVI Laser Corp.). In the dynamic anisotropy measurements, this filter combination was used in both detection channels in the T-format configuration.

All of the dynamic data were fitted by nonlinear least-squares (NLLS) analysis to various models, as discussed below. The best fits were judged on the basis of the χ^2 goodness-of-fit parameter, the randomness of the fitting residuals, and visual inspection of the fitting curve.

In the fluorescence lifetime determinations, the multifrequency phase and modulation data were fitted to a multiexponential decay law,

$$I(t) = \sum_{i=1}^{n} A_i \exp(-t/\tau_i) \tag{2}$$

using a Marquardt–Levenberg NLLS algorithm.[13] In eq 2, A_i and τ_i are the amplitude and the fluorescence decay time of the ith component, respectively. A solution of fluorescein (pH 7.5 phosphate buffer) served as the reference fluorophore. Under our experimental conditions, the fluorescence lifetime of the fluorescein reference was determined to be 4.02 ± 0.05 ns.

In the dynamic anisotropy measurements, the time-dependent anisotropy decay, $r(t)$, was calculated as

$$r(t) = \frac{I(t)_v - I(t)_h}{I(t)_v + 2I(t)_h} \tag{3}$$

where $I(t)_v$ and $I(t)_h$ represent the fluorescence intensity decays of the vertical and horizontal components of the emission beam that is excited with vertically polarized light. In the frequency domain, two measured quantities, phase angle difference (Δ) between the horizontal and the parallel components of the modulated emission,

$$\Delta = \phi_h - \phi_v \tag{4}$$

and the ratio (Λ) of the amplitudes of the modulated emission,

$$\Lambda = m_v/m_h \tag{5}$$

are used in the calculation of $r(t)$.[9,11,14]

The anisotropy data were fitted, using NLLS routines in software that was supplied with the instrument, to three different models, as described below.

(1) Isotropic rotator:

$$r(t) = r_0 \exp(-t/\Phi) \tag{6}$$

where Φ is the rotational correlation time and r_0 represents a limiting anisotropy for $t = 0$. An isotropic, or monoexponential, decay is expected for a spherical molecule when only one rotational motion contributes to the loss of polarization. Fluorescein free in solution is assumed to be pseudospherical and is considered to be an ideal isotropic rotator (r_0) because its absorption and emission dipole moments are parallel and only the rotation around one of the molecular axes will result in anisotropy loss.

(2) Anisotropic rotator:

$$r(t) = r_0 \sum_{i=1}^{n} \alpha_n \exp(-t/\Phi_n), \quad n = 2 \tag{7}$$

where Φ_n and α_n are the rotational correlation time and the associated amplitude of each of the decay components. The anisotropic rotator model is used to describe the multiexponential anisotropy decay of a molecule which does not exhibit equal rotational rates in all directions.[11,14–18]

(3) Hindered rotator:

$$r(t) = (r_0 - R_\infty) \sum_{i=1}^{n} \alpha_n \exp(-t/\Phi_n) + R_\infty, \quad n = 1 \tag{8}$$

The hindered rotator model, which is a monoexponential decay function with a constant factor, may be used to represent a limiting case of the more general model for an anisotropic rotator.[19] The term R_∞ describes a limiting anisotropy observed at times which are long compared to the fluorescence lifetime. If one of the rotational correlation times is much longer than the fluorescence lifetime, the contribution of the slow motion to the anisotropy loss becomes significant only when the anisotropy is not fully decayed by the fast component because of hindered rotation. Attempts have been made to connect the quantity R_∞ with a cone angle δ or an order parameter to describe the probe.[7,11]

For the determination of the anisotropy decay, the measured data were fitted to each of the three models. In most cases, only the rotational correlation times and the amplitudes were allowed to vary in the fits; the limiting anisotropy (r_0) of fluorescein was

(12) Mitchell, G.; Swift, K. In *Time-Resolved Laser Spectroscopy in Biochemistry II*; Lakowicz, J. R., Ed.; SPIE 1204; SPIE–The International Society for Optical Engineering: Bellingham, WA, 1990; Part 1, pp 270–274.

(13) *Globals Unlimited*, Technical reference manual; Laboratory for Fluorescence Dynamics, Department of Physics, University of Illinois, 1110 W. Green St., Urbana, IL 61801; 1990.

(14) Lakowicz, J. R.; Cherek, H.; Kusba, J.; Gryczynski, I.; Johnson, M. J. *J. Fluoresc.* **1993**, *3*, 103.

(15) Lakowicz, J. R.; Gryczynski, I.; Johnson, M. L. *Biophys. Chem.* **1994**, *52*, 1.

(16) Weber, G. *J. Chem. Phys.* **1971**, *55*, 2399.

(17) Weber, G.; Belford, G. G.; Belford, R. L. *Proc. Natl. Acad. Sci. U.S.A.* **1972**, *69*, 1392.

(18) Zannoni, C. *Mol. Phys.* **1981**, *42*, 1303.

(19) Lakowicz, J. R.; Maliwal, B. P.; Cherek, H.; Balter, A. *Biochemistry* *22*, **1983**, 1741.

Table 2. Steady-State Fluorescence Anisotropy Results for Set I and Set II Oligomers

sample	fluorescence anisotropy		
	ss	ds	ds+*Eco*RI
	Set I		
DNA28-6C-5′	0.037	0.056	0.073
DNA28-6C-mid	0.034	0.053	0.067
DNA28-6C-3′	0.040	0.044	0.053
	Set II		
DNA33-4C-5′	0.061	0.091	0.100
DNA33-6C-5′	0.049	0.076	0.106
DNA33-9C-5′	0.040	0.048	0.073
DNA33-12C-5′	0.038	0.060	0.055

fixed to a value of 0.40,[20] and the fluorescence lifetime was fixed to the experimentally determined value. In the few cases in which r_0 was allowed to vary, a limiting anisotropy of 0.40 was recovered from the fit.

RESULTS

Oligomer Samples. Two different sets of fluorescein-labeled DNA oligomers were used in the experiments. These are summarized in Table 1, which also gives the abbreviations used in this paper for the different oligomers. The sequences of the two sets are shown in Figure 2. Set I consists of 28-base oligomers (28-mers) in which the fluorescein was attached by a 6-carbon tether. In this sample set, the location of the binding site of the *Eco*RI enzyme was varied. Three different binding locations were investigated: 1 base from the 5′ end of the DNA strand (referred to as the 5′ binding site), 5 bases from the 5′ end (referred to as the middle binding site), and 11 bases from the 5′ end (referred to as the 3′ binding site). The second set of oligomers, set II, consists of 33-base oligomers (33-mers) in which the *Eco*RI binding site is located one base from the 5′ end and the length of the tether was varied. Oligomers with 4-, 6-, 9-, and 12-carbon tethers were used to attach the fluorescein to the oligomer. For each oligomer, four different samples were prepared: single-stranded DNA (ss), single-stranded DNA + *Eco*RI (ss+*Eco*RI), double-stranded DNA (ds), and double-stranded DNA + *Eco*RI (ds+*Eco*RI).

Steady-State Anisotropy. The steady-state anisotropy results are shown in Table 2. For the single strands, the anisotropy is greatest for the 4-carbon tether and decreases with increasing tether length. Anisotropy increases upon hybridization and again upon *Eco*RI binding to the double strand. The greatest increase is observed for the oligomers with the 6-carbon tether and the *Eco*RI binding site at the 5′ end, which is closest to the fluorescein label. The increase becomes smaller as the tether length is increased or as the *Eco*RI binding site is moved toward the 3′ end.

Fluorescence Lifetime Measurements. In order to perform DFA experiments, it is necessary to first analyze the fluorescence lifetime characteristics of the labeled oligomers. The fluorescence lifetime results are shown in Table 3 for set I (the oligomers with the *Eco*RI binding site in various positions) and in Table 4 for set II (the oligomers with different tether lengths). For most of the samples, the data were best fit by biexponential decays. In the other cases, monoexponential decays were indicated. For the biexponential decays, the shorter lifetime component generally contributed <5% of the total intensity and showed poor run-to-run reproducibility. Similar results for the dominant lifetime component, which is in the range of 3.8–4.3 ns, were obtained when the second lifetime component was allowed to float, as in the results presented in Tables 3 and 4, and when it was fixed to 0 ns to account for scattered light (results not shown). Therefore,

(20) Fleming, G. R.; Morris, J. M.; Robinson, G. W. *Chem. Phys.* **1976**, *17*, 91.

Table 3. Fluorescence Lifetime Results for Set I Oligomers[a]

	τ_1	A_1	τ_2	A_2	χ^2
		DNA28-6C-5′			
ss	3.83	0.98	0	0.02	4.2
ds	4.00	0.98	0	0.02	1.2
ss+*Eco*RI	3.87	0.97	0.43	0.03	1.2
ds+*Eco*RI	4.06	0.98	0.30	0.02	6.2
		DNA28-6C-mid			
ss	4.07	0.98	0.67	0.02	1.7
ds	4.26	0.97	1.36	0.03	2.3
ss+*Eco*RI	4.06	0.98	0.44	0.02	1.8
ds+*Eco*RI	4.26	0.97	1.28	0.03	2.4
		DNA28-6C-3′			
ss[b]	4.15	0.81	3.56	0.19	1.4
	4.03	1			1.7
ds	4.04	0.98	0.60	0.02	1.7
ss+*Eco*RI	4.09	0.98	1.50	0.02	0.8
ds+*Eco*RI	4.08	0.98	1.34	0.02	1.1

[a] In cases where the biexponential fit revealed a second component with a fluorescence lifetime comparable to that of the main lifetime component, the results of a monoexponential fit are also shown. Standard deviations of triplicate determinations of τ_1 were <3%. τ is the fluorescence lifetime (ns), A is the fractional intensity contribution, and χ^2 is a goodness-of-fit parameter. [b] Fits to both two-component and one-component models are shown.

Table 4. Fluorescence Lifetime Results for Set II Oligomers[a]

	τ_1	A_1	τ_2	A_2	χ^2
		DNA33-4C-5′			
ss	3.92	0.94	1.46	0.06	1.1
ds	3.86	0.84	1.06	0.16	4.5
ss+*Eco*RI	3.90	0.95	1.36	0.05	1.5
ds+*Eco*RI	3.87	0.84	0.96	0.16	3.0
		DNA33-6C-5′			
ss	3.97	0.97	0.49	0.03	2.3
ds	4.05	0.99	0.18	0.01	1.2
ss+*Eco*RI	3.95	0.97	0.53	0.03	1.4
ds+*Eco*RI	4.13	0.98	1.40	0.02	1.4
		DNA33-9C-5′			
ss	4.05	0.99	0.13	0.01	1.3
ds	4.01	0.99	0.19	0.01	0.8
ss+*Eco*RI	4.07	0.98	0.23	0.02	1.0
ds+*Eco*RI	4.05	0.97	0.32	0.03	1.2
		DNA33-12C-5′			
ss[b]	4.12	0.89	2.74	0.11	1.0
	3.95	1			3.8
ds	3.97	0.99	0.19	0.01	0.9
ss+*Eco*RI[b]	4.07	0.95	2.42	0.05	0.9
	3.97	1			4.4
ds+*Eco*RI	4.04	0.97	0.39	0.03	1.1

[a] In cases where the biexponential fit revealed a second component with a fluorescence lifetime comparable to the main lifetime component, the results of a monoexponential fit are also shown. Standard deviations of triplicate determinations of τ_1 were <3%. τ is the fluorescence lifetime (ns), A is the fractional intensity contribution, and χ^2 is a goodness-of-fit parameter. [b] Fits to both two-component and one-component models are shown.

Table 5. Dynamic Fluorescence Anisotropy Results for Set I Oligomers[a]

	isotropic		anisotropic					hindered		
	Φ	χ^2	Φ_1	α_1	Φ_2	α_2	χ^2	Φ	R_∞	χ^2
					DNA28-6C-5′					
ss	0.61	82.2	0.51	0.97	∞	0.03	3.6	0.51	0.012	3.3
ds	0.87	258.9	0.63	0.92	25	0.08	9.0	0.66	0.026	9.9
ss+*Eco*RI	0.63	69.2	0.53	0.96	∞	0.04	8.6	0.53	0.013	5.1
ds+*Eco*RI	0.97	681.5	0.57	0.88	23	0.12	4.9	0.62	0.038	8.9
					DNA28-6C-mid					
ss	0.51	142.9	0.38	0.95	23	0.05	1.7	0.40	0.015	2.6
ds	0.68	395.4	0.41	0.86	13	0.11	1.7	0.46	0.028	9.5
ss+*Eco*RI	0.56	99.6	0.46	0.96	59	0.04	4.2	0.46	0.015	4.1
ds+*Eco*RI	0.76	411.6	0.47	0.90	16	0.10	2.4	0.52	0.029	7.9
					DNA28-6C-3′					
ss	0.37	3.5	0.37	1			4.4	0.37	−0.002	3.6
ds	0.62	148.5	0.36	0.84	4	0.16	1.9	0.49	0.021	23.4
ss+*Eco*RI	0.39	2.7	0.39	1			2.9	0.39	−0.001	2.6
ds+*Eco*RI	0.69	141.9	0.44	0.86	5	0.14	2.4	0.55	0.018	12.2

[a] Fits are shown to three decay models: the isotropic rotator, the biexponential anisotropic rotator, and the hindered rotator. For each sample, a single fluorescence lifetime (from Table 3) was used in the DFA analysis. Φ is the rotational correlation time (ns), α is the fractional intensity contribution, χ^2 is a goodness-of-fit parameter, and R_∞ is the limiting anisotropy at "infinity". Standard deviations of triplicate determinations of Φ_1 or Φ were <10%, and standard deviations of the fractional intensities of Φ_1 were <5%.

Table 6. Dynamic Fluorescence Anisotropy Results for Set II Oligomers[a]

	isotropic		anisotropic					hindered		
	Φ	χ^2	Φ_1	α_1	Φ_2	α_2	χ^2	Φ	R_∞	χ^2
					DNA33-4C-5′					
ss	0.62	1238	0.41	0.87	12.3	0.13	1.8	0.47	0.035	27.2
ds	1.14	522	0.72	0.83	10.9	0.17	6.5	0.83	0.042	21.9
ss+*Eco*RI	0.86	71	0.45	0.78	4.0	0.22	1.2	0.65	0.026	11.9
ds+*Eco*RI	1.02	102	0.52	0.72	5.5	0.29	0.5	0.77	0.049	11.9
					DNA33-6C-5′					
ss	0.74	73	0.62	0.96	∞	0.04	6.9	0.62	0.018	6.3
ds	0.92	270	0.68	0.91	25	0.09	8.4	0.71	0.027	9.0
ss+*Eco*RI	0.89	150	0.69	0.94	∞	0.06	13.5	0.68	0.023	12.0
ds+*Eco*RI	1.24	727	0.70	0.85	37	0.15	8.6	0.74	0.052	10.2
					DNA33-9C-5′					
ss	0.33	22	0.31	0.99	99.2	0.01	26.0	0.38	−0.011	1.9
ds	0.39	11	0.39	1			11.8	0.43	−0.008	2.3
ss+*Eco*RI	0.38	31	0.38	1			31.8	0.43	−0.011	2.9
ds+*Eco*RI	0.53	7	0.48	0.97	5.5	0.03	3.3	0.5	0.005	3.7
					DNA33-12C-5′					
ss	0.32	18	0.32	0.99	99.2	0.01	18.9	0.36	−0.011	0.7
ds	0.36	9	0.36	0.99	99.1	0.01	9.2	0.39	−0.006	4.0
ss+*Eco*RI	0.36	2	0.36	1			1.7	0.36	0.000	1.7
ds+*Eco*RI	0.49	4	0.48	0.99	95	0.01	3.4	0.48	0.001	3.4

[a] Fits are shown to three decay models: the isotropic rotator, the biexponential anisotropic rotator, and the hindered rotator. For each sample, a single fluorescence lifetime (from Table 4) was used in the DFA analysis. Φ is the rotational correlation time (ns), α is the fractional intensity contribution, χ^2 is a goodness-of-fit parameter, and R_∞ is the limiting anisotropy at "infinity". Standard deviations of triplicate determinations of Φ_1 or Φ were <10%, and standard deviations of the fractional intensities of Φ_1 were <5%.

it is most likely that the second lifetime component is an artifact caused by small amounts of scattered light and noise. A possible exception is the hybridized oligomer with the 4-carbon tether, which may have a significant second decay component. Further studies would be needed to verify such biexponential decay. In this work, only the dominant lifetime was used in the analysis of the DFA data for all samples.

For the single strands, slight increases in lifetime were observed when the *Eco*RI binding site was moved away from the 5′ end or when the tether length was increased. Hybridization causes small but reproducible increases in lifetime for the oligomers that have a 6-carbon tether and in which the *Eco*RI binding site is in the 5′ or middle position, but it has no effect on the other oligomers. Addition of *Eco*RI has no significant effect on the lifetimes in any of the samples.

Dynamic Fluorescence Anisotropy. The DFA results are shown in Tables 5 and 6 for the set I and set II oligomers, respectively. The data for both sets of samples were evaluated by three different models: the isotropic rotator, the anisotropic rotator with two rotational correlation times (Φ_1, Φ_2), and the hindered rotator. Fits to an anisotropic rotator with three rotational correlation times (not shown) gave no improvement over the two-component anisotropic rotator model and recovered a zero fractional intensity for the third correlation time.

In most cases, the experimental data could be reasonably fit (based on the random residual distribution and the χ^2 values) by either the biexponential anisotropic rotator or the hindered rotator model, yielding similar values for the rotational correlation time Φ_1 of the anisotropic rotator model and rotational correlation time Φ of the hindered rotator model. There is, however, an interesting relationship between the goodness-of-fit to the different models and the length of the fluorescein tether. For the shortest (4-carbon) tether, the biexponential anisotropic rotator gives the best fit, while for the long (9- and 12-carbon) tethers, the hindered rotator model generally gives the best fits (in a few cases for the long tethers, the isotropic model gave results that were comparable to one or both of the other models). For the 6-carbon tether, the data are fit equally well by the anisotropic rotator and the hindered rotator models. This trend from biexponential, anisotropic behavior for short tethers to hindered rotator behavior for long tethers is discussed later.

In the anisotropic rotator model, Φ_1 is largest for the single strand when the *Eco*RI binding site is at the 5′ position and when the tether length is 6 carbons. Similar trends are observed for Φ in the hindered rotator model. The fractional intensity contribution of Φ_2 is small (<6%), except for the 4-carbon tether. In the anisotropic rotator model, hybridization generally causes increases in both Φ_1 and the fractional intensity of Φ_2. In the hindered rotator model, hybridization similarly increases both Φ and R_∞. This effect is largest for the shorter tether lengths. For the oligomers with the binding site at the 5′ end and a tether length of 4 or 6 carbons, there is an additional increase in the contribution of Φ_2 upon addition of *Eco*RI. For the longer tethers, the fractional contribution of Φ_2 is negligible, and in some cases, the isotropic model is sufficient to describe the data; much less hindrance is observed in these samples compared to the shorter tethers.

DISCUSSION

Under the experimental conditions of these studies (pH = 7.5), the dianionic form of fluorescein predominates. It is known that fluorescein does not intercalate in DNA,[21] and its fluorescence characteristics are relatively insensitive to environmental conditions other than pH. In experiments with free fluorescein in the presence of unlabeled oligomers (results not shown), both single-

(21) Murakami, A.; Nakaura, M.; Nakatsuji, Y.; Nagahara, S.; Tran-Cong, Q.; Makino, K. *Nucleic Acids Res.* **1991**, *19*, 4097.

stranded and double-stranded, no changes in the fluorescence lifetime or anisotropy decay were detected.

The fluorescence decay of the covalently tethered fluorescein is essentially monoexponential. A small increase in lifetime is observed upon hybridization for oligomers with the 6-carbon tether. For the other oligomers, the lifetimes remained essentially constant. *Eco*RI binding had no effect on the lifetimes of any of the oligomers. The unique sensitivity of the fluorescence lifetimes of the 6-carbon tether oligomers to hybridization, as well as the observation of maximum increases in anisotropy for these oligomers upon hybridization and *Eco*RI binding, clearly indicates that the 6-carbon tether length is particularly well-suited to detection of hybridization and *Eco*RI enhanced detection.

For all of the oligomers, the main anisotropy decay can be attributed to a fast rotational motion that is evident in all of the models used to fit the DFA data. This rotation occurs on the time scale of a few hundred picoseconds (~350–700 ps). This is only slightly longer than the rotational correlation time of ~0.2 ± 0.05 ns which was determined for free fluorescein in solution under similar conditions of pH and viscosity.

For the oligomers with the long tethers (9 and 12 carbons), the motion of the fluorescein is not coupled to the motion of the oligomer because of the large freedom of motion afforded by the long tether. This nearly independent motion results in rotation that is essentially isotropic. For the shorter tethers (4 and 6 carbons), the fluorescein rotational motion is more influenced by the attached oligomer, and the biexponential anisotropy decay model provides good representation of the rotational motion. The rotational correlation time of the second, slow motion varies from 10 ns to "infinity". Thus, although two rotational decay components were clearly indicated for the oligomers with shorter tethers, recovery of a value for the second correlation time (Φ_2) was markedly unstable. This is because the fluorescence lifetime is much shorter than Φ_2.

To further examine the instability of Φ_2, a simulation of an anisotropic rotator was conducted in which the rotational correlation times were similar to the ones found in our experiments (Φ_1 = 0.5 ns, Φ_2 = 20 ns). These simulated data sets were used to monitor the dependence of the goodness of fit (expressed as the χ^2 values) on the long rotational correlation time Φ_2. As shown in Figure 3, it is difficult even for this simulation to recover an exact value for Φ_2, especially for the case in which Φ_2 is much longer than τ_f and has only a small fractional intensity. For comparison, a third data set was simulated with the same parameter settings as for the previous simulations except that Φ_2 was set to 4 ns. In this case, the fits are much more sensitive to the value of Φ_2.

Despite the uncertainties in the actual magnitude of Φ_2, its existence can be used to explain the significant increases in the steady-state anisotropy that are observed upon hybridization of some oligomers, just as the absence of a significant Φ_2 can explain the absence of a significant increase in steady-state anisotropy for other oligomers. This effect is illustrated in Figure 4 using a modified form of the Perrin equation to describe the dependence of the steady-state anisotropy (r) on Φ_2 and the ratio of the fractional intensities[19] of Φ_1 and Φ_2:

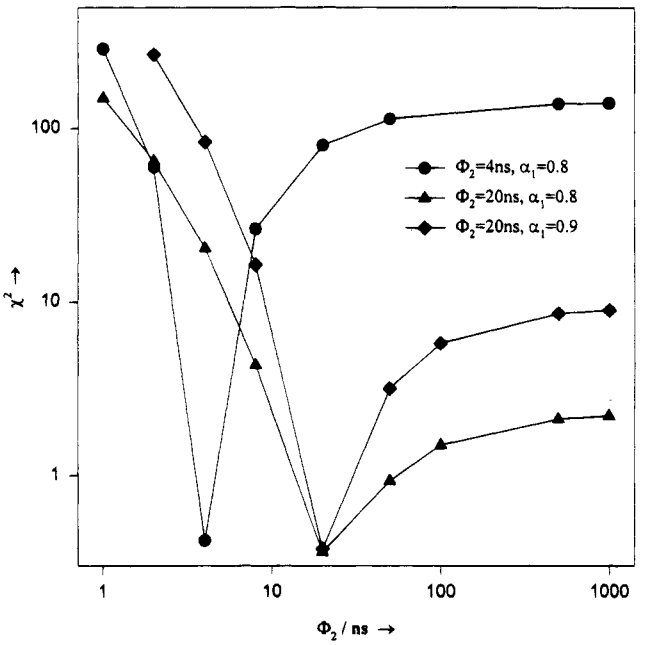

Figure 3. Simulated χ^2 for an anisotropic rotator with two rotational correlation times. Three initial data sets were simulated and used for the χ^2 calculations (for all, r_0 = 0.4, τ_f = 4 ns, Φ_1= 0.5 ns): (▲) Φ_2 = 20 ns, α_1 = 0.8, α_2 = 0.2; (◆) Φ_2 = 20 ns, α_1 = 0.9, α_2 = 0.1; and (●) Φ_2 = 4 ns, α_1 = 0.8, α_2 = 0.2. A constant phase error of 0.5° and a constant modulation error of 0.005 were assumed.

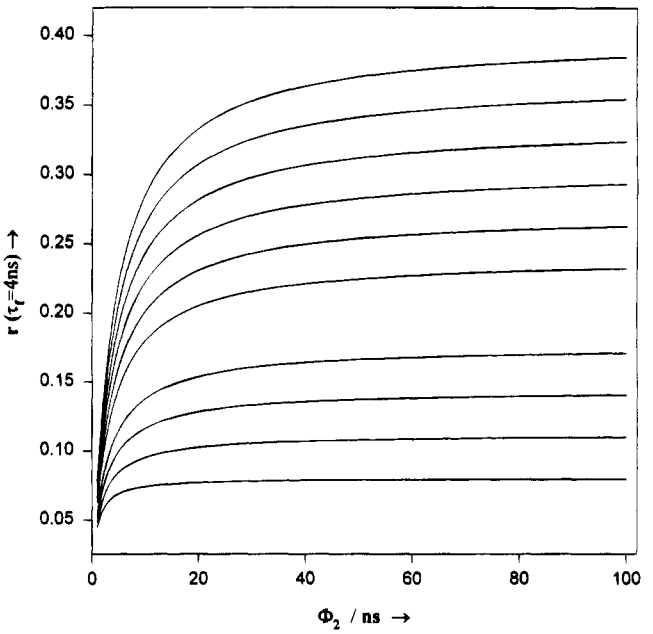

Figure 4. Steady-state anisotropy (r) simulated for an anisotropic rotator with two rotational correlation times (Φ_1=1 ns) for different fractional contributions of Φ_2 (α_2 = 0.001, 0.1, 0.2, 0.3, 0.5, 0.6, 0.7, 0.8, 0.9, and 0.999, from bottom to top).

$$r = \frac{\alpha r_0}{1 + (1/\Phi_1 + 1/\Phi_2)\tau_f} + \frac{(1 - \alpha)r_0}{1 + (\tau_f/\Phi_2)} \qquad (9)$$

As stated above, it is difficult to determine a reliable value for Φ_2 because it is much longer than the fluorescence lifetime. On the other hand, this allows us to reduce the number of fitting parameters and thereby simplify the model used to fit the data. It is reasonable to assume that during the fluorescence lifetime, the fast component is primarily responsible for the anisotropy decay, and because of a hindrance, the anisotropy does not decay to zero.

The longer decay component can be represented in a first approximation by a constant term, R_∞. This can be modeled as a hindered rotator. Application of this model to the DFA data produced results that were similar to the steady-state anisotropy results. R_∞ increases upon hybridization and increases further upon *Eco*RI binding to the double strand if the binding site is near the 5′ end. Similar increases in R_∞ are observed for the 4C and 6C tether lengths. This tendency is less pronounced for the 9C and 12C tethers.

CONCLUSIONS

The results demonstrate the detection of DNA hybridization by fluorescence anisotropy. The detection can be improved by including a binding site for the enzyme *Eco*RI on the oligomer probe. *Eco*RI, which binds only to double-stranded DNA, increases the effective volume of the double strand complex and thereby amplifies the difference between the anisotropies of the single strand and the double strand. *Eco*RI enhancement of polarization can be applied to the detection of any sequence when used in conjunction with a nucleic acid amplification method such as polymerase chain reaction (PCR) or strand displacement amplification (SDA). The approach involves the use of an amplification primer or detector probe that contains the specific target sequence at its 3′-end and the *Eco*RI site at its 5′-end. The primer or detector probe is converted from a single strand to a double-stranded form that binds *Eco*RI during amplification of the target sequence.[22]

The results show that the *Eco*RI-enhanced polarization detection scheme is effective only if (1) the fluorescein tether is short (~6 carbons or less) and (2) the *Eco*RI binding site is near the fluorescein attachment site at the 5′ end. The 6C tether is the optimal length for the particular system investigated here, yielding the largest anisotropy differences upon hybridization in both the absence and the presence of *Eco*RI binding. Further investigations are needed to determine the dependence of the optimium tether length on the sequence and length of the probe, the dye used for detection, and the location of the *Eco*RI binding site.

The anisotropy decay in the single strand is dominated by the very fast motion of the fluorescein molecule about the tether. Only a very small portion, if any, of the anisotropy decay is caused by motion of the whole molecular unit (oligomer + fluorescein). For the oligomers with a short (4 or 6 carbons) tether, the contribution of the slow rotational component to the anisotropy decay increases upon hybridization and further upon binding of *Eco*RI to the double strand near the 5′ end, due to hindrance of the fast fluorescein motion, and the anisotropy does not decay to zero. When the tether length is increased, the motion of the fluorescein is less influenced by hybridization and *Eco*RI binding, and anisotropy decay is due to the fast motion of the fluorescein only.

ACKNOWLEDGMENT

The authors are grateful to Michael Mitchell of Becton Dickinson and Co. Research Center for performing the molecular modeling of the *Eco*RI bound to the fluorescein-labeled DNA oligomer and providing the graphical depiction of this system that is shown in Figure 1.

Received for review May 17, 1995. Accepted August 13, 1995.[⊗]

AC950478Z

(22) Walker, G. T.; et. al., unpublished results.

(23) Kim, Y.; Grable, J. C.; Love, R.; Greene, P. J.; Rosenberg, J. M. *Science* **1990**, *249*, 1307.

(24) Bernstein, F. C.; Koetzle, T. F.; Williams, G. J. B.; Meyer, E. F., Jr.; Brice, M. D.; Rodgers, J. R.; Kennard, O.; Shimanouchi, T.; Tasumi, M. *J. Mol. Biol.* **1977**, *112*, 535.

(25) Abola, E. E.; Bernstein, F. C.; Bryant, S. H.; Koetzle, T. F.; Weng, J. In *Scientific Applications*; Allen, F. H., Bergerhoff, G., Sievers, R., Eds; Data Commission of the International Union of Crystallography: Bonn/Cambridge/Chester, 1987; pp 107–132.

[⊗] Abstract published in *Advance ACS Abstracts,* September 15, 1995.